10-nm-wide Tunable In-series Laser Array with High single-mode Stability

Zhenxing Sun[1], Rulei Xiao[1,*], Zhirui Su[1], Gen lv[1], Zhao Chen[2], Jilin Zheng[1], Yunshan Zhang[1], Jun Lu[1], Yuechun Shi[1,4], Yi-Jen Chiu[3], and Xiangfei Chen[1]

[1]Key Laboratory of Intelligent Optical Sensing and Manipulation of the Ministry of Education & National Laboratory of Solid State Microstructures & College of Engineering and Applied Sciences & Institute of Optical Communication Engineering, Nanjing University, Nanjing 210093, Jiangsu, China

[2]School of Electronic and Electrical Engineering, Wuhan Textile University, Wuhan, 430073, P.R. China

[3]Institute of Electro-Optical Engineering and Semiconductor Technology Research Development Center, National Sun Yat-Sen University, Kaohsiung 80424, Taiwan, R.O.C.

[4]Nanjing University (Suzhou) High-Tech Institute, Suzhou 215123, China

**xrl@nju.edu.cn*

Abstract: We report a 10-nm-wide tunable in-series DFB laser array with high wavelength-spacing uniformity and high single-mode stability, which is guaranteed by high-precision control of grating phase error through reconstruction-equivalent-chirp technique.

OCIS codes: (140.0140) Lasers and laser optics; (140.3290) Laser arrays; (060.4510) Optical communications

1. Introduction

Wavelength-tunable semiconductor lasers are important components for future reconfigurable DWDM systems, which are expected to be massively applied in datacenters, metro-transport and access networks [1]. Recently, in 5G fronthaul applications, a key technology is the WDM-PON, where low-cost tunable lasers with 12-channel 100-GHz-spacings (~10 nm) are in great demand [2]. For such an application, there are mainly two types of tunable lasers, the tunable DBR laser, and the tunable DFB laser array. For the tunable DBR laser, wavelength control is an inherent issue that "mode hops" occur due to misalignment of the DBR and cavity modes and has long been a major question as to their suitableness for optical networks [3]. For the tunable DFB laser array, the lasing mode is very stable, but the intrinsic power loss induced by the N-to-1 combiner is undesirable [4]. At the same time, high wavelength-spacing uniformity DFB lasers are required to avoid large temperature tuning range.

Therefore, the MLAs are expected to be placed in series to avoid the insertion loss of the combiner. However, in this way, the single-mode stability and wavelength reliability are poor due to the reflection of the gratings of other lasers. This phenomenon is getting worse when the wavelength spacing is comparable with the bandgap of a laser's grating (typically 2-3 nm). But to avoid large temperature tuning range of a single laser, the wavelength spacing could not be too large.

In this paper, we proposed an in-series tunable 4-laser-array with wavelength spacings of 2.5 nm. Each DFB laser is designed as a three-section structure for better single-mode property. High single-mode stability and high wavelength-spacing uniformity are guaranteed by precise control of grating phase error by the reconstruction-equivalent-chirp (REC) technique. Based on our statistics from 40 laser arrays (160 lasers), wavelength deviations of 90.6% lasers are within ±0.2 nm, and SMSRs of 96.3% lasers are above 45 dB. The laser's output power is above 10 mW, and tunable 24 channels with 50-GHz-spacing were obtained with less than 20 °C temperature tuning range.

2. Device design

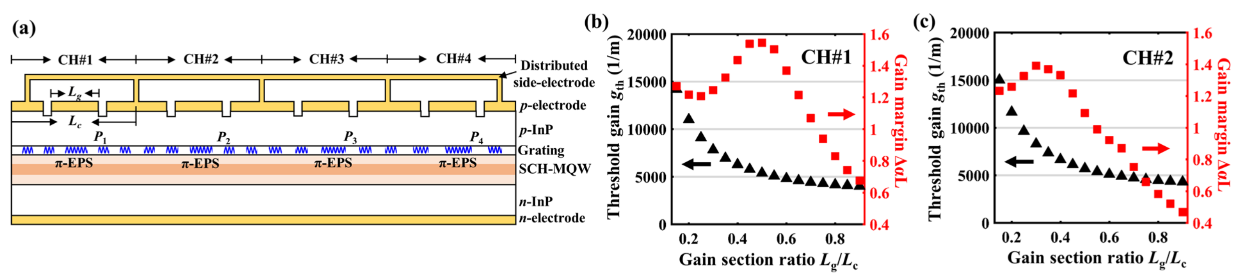

Fig. 1 (a) Schematic of the proposed tunable in-series laser array. Simulated threshold gain and gain margin of (b) CH#1, and (c) CH#2. (CH: channel, π-EPS: π equivalent phase shift, L_g: length of the gain section, L_c: length of a laser for one channel.)

A novel three-section π phase-shifted DFB laser is applied in our devices. The middle section is applied with a large current for optical gain and side sections are applied with small currents for near-transparent operations. The π phase shift is equivalently realized by REC technique. As shown in Fig. 1(a), 4 three-section lasers are placed in series in the tunable laser, and all the *p*-electrodes of distributed side sections are connected to a single pad for simple measurement. We also simulated the laser performance with different gain section ratio L_g/L_c, where L_g is the length of the gain section and L_c is the length of a laser for one channel. Owing to the symmetry of the structure, we just simulated for channel 1 (CH#1) and channel 2 (CH#2). As shown in Fig. 1(b) and (c), the threshold gains decrease in both channels with the increase of L_g/L_c owing to longer gain section. The highest gain margins are obtained when the gain section ratios are 0.5 and 0.3, respectively. In our design, the L_g/L_c is set at 0.5.

In the device, the precise control of the grating phase error is guaranteed by the REC technique [5]. Only common μm-level photolithography and holographic exposure are required during the grating fabrication. The grating phase error is reduced by a factor of $(P/\Lambda_0+1)^2$, which is usually more than two orders of magnitude. Here P is the sampled period, and Λ_0 is the seed grating period. In the proposed structure, this factor is approximately 555. Four sampling periods of P_1, P_2, P_3, and P_4 are designed for CH#1, #2, #3 and #4, respectively.

3. Device characterization

Figure 2(a) shows the microscopic top view of the proposed laser. The length of each channel is 600 μm and the gain section ratio is 0.5. A short 200-μm SOA is integrated in front for power equalization. Front and rear facets are both anti-reflection coated. The laser chip was mounted on a sub-mount, the temperature of which was controlled at 20 ℃ via the TEC. The optical spectra were recorded by the AQ6370 optical spectrum analyzer. Lasing spectra of 4 randomly-selected lasers are shown in Fig. 1(b-e), which shows good single-mode property and wavelength spacing uniformity. The current injected to the gain section, SOA, and distributed side-electrode are 60.0, 30.0, and 30.0 mA, respectively. When one channel is lighted, the gain electrode in front is injected with an appropriate current (transparent current) to compensate the material absorption. Here, the transparent current is 15 mA.

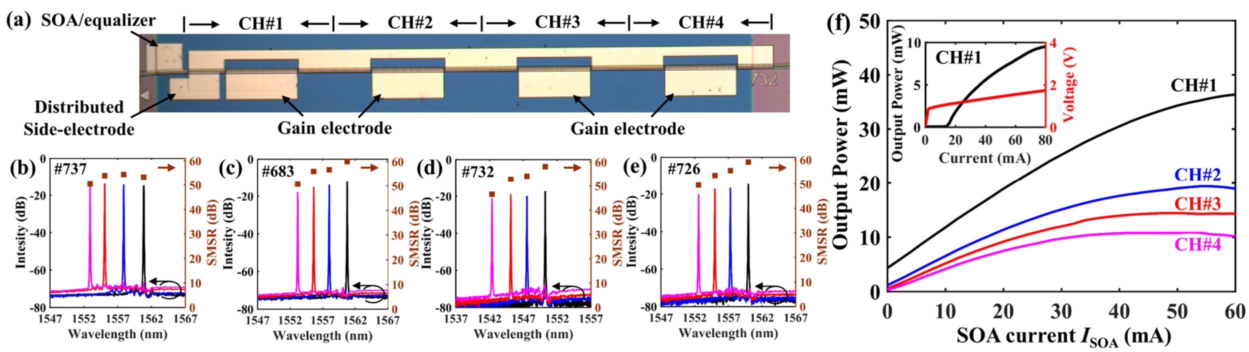

Fig. 2 (a) Microscopic top view of the in-series laser array. (b-e) Lasing spectra of 4 randomly-selected laser array. (f) For #726 laser, the output power of 4 channels when the SOA current is varied from 0 to 60 mA. The inset of (f) shows a P-I-V curve of CH#1.

Then we studied a randomly-selected laser (#726) in detail. As shown in the inset of Fig. 1(f), the threshold of CH1 is 17.2 mA. By changing the SOA current, different output powers are obtained for the 4 channels. The output power of CH#4 is lowest due to the transmission loss from the in-front sections. The output power of 10.0 mW can be obtained in the CH#4 with a SOA current of 34.5 mA.

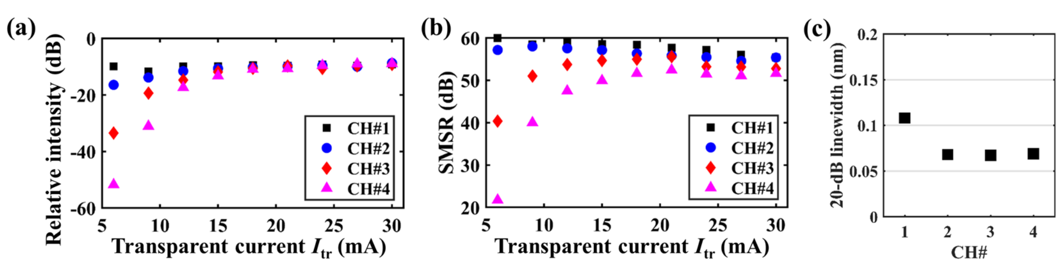

Fig. 3 For laser #726, the (a) relative intensity and (b) SMSR when the transparent current is varied from 5 to 30 mA. (c) 20-dB linewidth of the four channels of the laser.

The obvious drop of power from CH#1 to #4 in Fig. 2(f) is due to the low transparent current. However, an increase of the transparent current will lead to bad single-mode property owing to the increased material gain. Therefore, to find the optimal transparent current, we recorded the optical intensity and the optical SMSRs of all the four channels under different transparent currents. As shown in Fig. 3(a), the optical intensity is balanced for four channels when the transparent current is above 20 mA. But the SMSRs are getting worse when the transparent current grows above 20 mA. As a result, the optimal transparent current is regarded as 20 mA. In addition, the 20-dB linewidth is measured as shown in Fig. 3(c).

We linearly fitted the lasing wavelengths of the four channels of all 40 tunable laser arrays and made statistics of the wavelength deviation, the average wavelength spacing (fitting slope) and the SMSRs. As is shown in Fig. 4(a), the 97.5%, 87.5%, 87.5, and 90% of the wavelength deviations of CH#1, #2, #3, and #4, respectively, are within ±0.2 nm. As shown in Fig. 4(b), 62.5% of the fitting slopes are between 2.4 nm and 2.6 nm. Figure. 4(c) shows the SMSRs of the four channels in the measured 40 tunable laser arrays, among which only three channels work with SMSR below 40 dB.

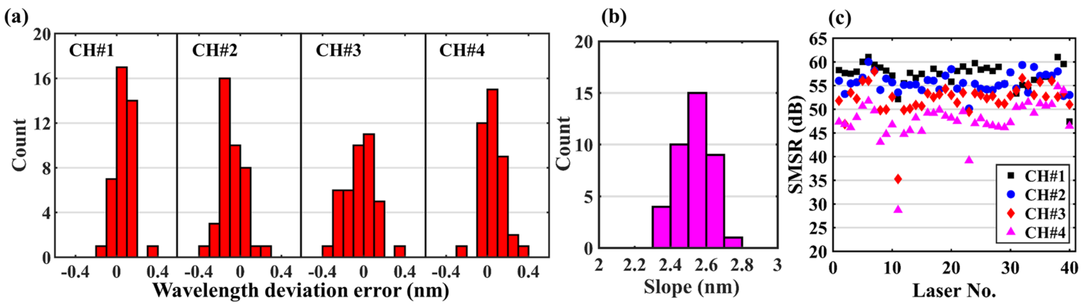

Fig. 4 (a) Linear-fitted wavelength deviation error of CH#1, #2, #3 and #4 of 40 tunable laser arrays. (b) Linear-fitted slopes, and (c) SMSRs of 40 tunable laser arrays.

For each tunable laser array, 24 channels with 50-GHz-spacing can be obtained by changing the temperature of the TEC. The SOA current is adjusted for balanced output power. The superimposed spectra of the 24 channels of laser #726 are shown in Fig. 5(a). The corresponded temperatures and SMSRs of all the channels are shown in Fig. 5(b). The max temperature tuning range is only 18.2 ℃ owing to the precise wavelength control.

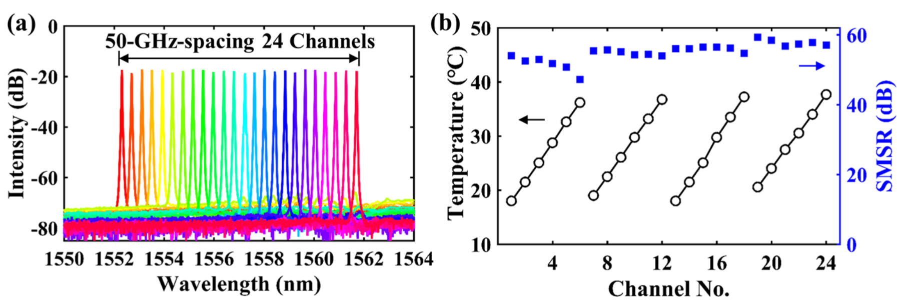

Fig. 5 (a) Superimposed spectra of the 24 channels with 50-GHz-spacing. (b) Temperatures of the TEC and the SMSRs of the 24 channels.

4. Conclusion

We proposed a tunable in-series laser array with a 10-nm-wide tuning range. Based on the high precision control of grating phase error and the three-section design of each DFB laser, high single-mode stability and high wavelength-uniformity are obtained. Based on our statistics of 40 laser array (160 lasers), 90.6% of the wavelength deviations of all the channels are within ±0.2 nm and 96.3% of the SMSRs of all the channels are above 45 dB. 24 channels with 50-GHz-spacing are obtained with a temperature tuning range of only 18 ℃.

Funding

Chinese National Key Basic Research Special Fund (2017YFA0206401); Science and Technology Project and Natural Science Foundation of Jiangsu province (BE2017003-2, BK20160907); National Natural Science Foundation of China (61435014 and 11574141); Suzhou technological innovation of key industries (SYG201844).

References

[1] K. Grobe, et al., J. Light. Technol., vol. 32, no. 16, pp. 2815–2823, 2014.
[2] C. Wagner, et al., J. Light. Technol., vol. 34, no. 22, pp. 5300–5307, 2016.
[3] G. A. Fish, et al., Conf. Opt. Fiber Commun. Tech. Dig. Ser., vol. 54, no. 2, pp. 1–4, 2001.
[4] H. Ishii, et al., IEEE J. Sel. Top. Quantum Electron., vol. 13, no. 5, pp. 1089–1094, 2007.
[5] Y. Shi, et al., J. Light. Technol., vol. 31, no. 20, pp. 3243–3250, 2013.